0038-075C/99/1648-527-541
Soil Science

August 1999
Vol. 164, No. 8
Printed in U.S.A.

TECHNICAL ARTICLES

ESTIMATION OF SOIL HYDRAULIC PROPERTIES WITH THE CONE PERMEAMETER: FIELD STUDIES

Radka Kodešová[1], Sondra E. Ordway[1], Molly M. Gribb[1] and Jiří Šimůnek[2]

We present field application of the cone permeameter method for estimating soil hydraulic properties: the soil-moisture characteristic curve, $\theta(h)$, and the hydraulic conductivity function, $K(h)$. The cone permeameter was designed to inject water into the soil under known pressure. The cumulative inflow volume and pressure heads measured with tensiometer rings at two locations above the water source are recorded in time. The observed data sets are analyzed using an inverse modeling method to predict the soil hydraulic properties. The device was field-tested for the first time in two types of sandy soil. Tests were always conducted with two sequentially applied pressure heads of different magnitudes for different experimental runs. After the water source was shut off, tensiometer measurements were continued to monitor the redistribution of water in the soil. To study the impact of one or two steps of applied pressure head on estimates of wetting soil hydraulic properties, we carried out numerical inversions for data from the injection (wetting) part of experiment, first with only one supply pressure head and then with two supply pressure heads. For selected tests we analyzed data from the entire experiment to investigate hysteresis of the soil hydraulic properties. The resulting soil hydraulic properties correspond well with those obtained with standard techniques. (Soil Science 1999;164:527–541)

Key words: Inverse solution, cone permeameter, soil hydraulic properties, unsaturated hydraulic conductivity function, soil-moisture characteristic curve, field studies.

THE soil-moisture characteristic, $\theta(h)$, and hydraulic conductivity, $K(h)$, curves are two basic hydraulic properties of soils. Current direct laboratory and *in situ* methods for their determination are often time consuming and costly. Parameter optimization is an indirect approach that makes it possible to obtain $K(h)$ and $\theta(h)$ simultaneously from transient flow data (Kool et al. 1987). In this case, a flow event is modeled with an appropriate governing equation and analytical expressions of $K(h)$ and $\theta(h)$. The unknown parameters of $K(h)$ and $\theta(h)$ are obtained by minimization of an objective function describing the differences between some measured flow variables and those simulated with a numerical flow code. This methodology was originally applied to laboratory one-step (Kool et al. 1985; Parker et al. 1985; van Dam et al. 1992; Wildenschild et al. 1997) and multi-step (van Dam et al. 1994; Eching and Hopmans 1993; Eching et al. 1994; Zurmühl and Durner 1998) outflow data. Parameter estimation has also been used with data obtained using the evaporation method (see, for example, Santini et al. (1995); Ciollaro and Romano (1995); Šimůnek et al. (1998b)). For field deter-

[1]Department of Civil & Environmental Engineering, University of South Carolina, 300 Main St., Columbia, SC 29208. Dr. Gribb is corresponding author. E-mail: gribb@sc.edu

[2]U.S. Salinity Laboratory, USDA-ARS, 450 W. Big Spring Rd., Riverside, CA 92507.

Received Jan. 12, 1999; accepted April 16, 1999.

mination of soil hydraulic properties, parameter estimation methods were applied to ponded infiltration flow data (Russo et al. 1991; Bohne et al. 1993), and tension disc infiltrometer flow data (Šimůnek and van Genuchten 1996, 1997; Šimůnek et al. 1998a). Another field technique for gaining information about the soil hydraulic properties via multi-step soil water extraction and parameter optimization was developed by Inoue et al. (1998). Both the tension disc infiltrometer and multi-step soil water extraction experiments are applicable only in the near surface. Gribb (1996) proposed a new cone penetrometer tool (e.g., cone permeameter) and use of parameter optimization to estimate soil hydraulic properties at depth. A prototype was further developed by Leonard (1997). A detailed description of the prototype as well as its use under saturated and unsaturated conditions were previously presented by Gribb et al. (1998). The cone permeameter was designed to inject water under known pressure into the soil. The cumulative inflow volume and pressure heads at two locations above the source are measured during the injection (wetting) part of experiment. Only the pressure heads are recorded during the redistribution process after the water supply is shut off. The prototype was previously tested in the laboratory aquifer. Kodešová et al. (1998, 1999) discussed results of the numerical analysis of data from the wetting parts of one-step applied pressure head cone permeameter experiments, which were performed in the laboratory for one soil type but under different initial and boundary conditions. They discovered that higher applied pressure head and lower initial pressure head conditions resulted in higher values of saturated soil moisture content, θ_s, and saturated hydraulic conductivity, K_s. They also studied the influence of cone permeameter placement (pushed vs. buried) on estimates of soil hydraulic properties and the possibility of including soil moisture content information into the optimization process. They found that soil densification caused by pushing the prototype to the testing depth resulted in slightly lower values of θ_s and K_s. They also showed that additional measurements of soil moisture content would be useful for more precise estimation of θ_s. Šimůnek et al. (1999) and Kodešová et al. (1999) examined both the wetting and redistribution parts of cone permeameter experiments to determine the wetting and drying branches of the soil hydraulic properties. In cases where the parameter θ_s was overestimated, they investigated the potential for optimization of additional parameters, such as the pore connectivity parameter in Eq. (8) (see below) and the anisotropy factor (expressing the ratio between horizontal and vertical K_s values), to obtain better fits of measured flow responses when θ_s was fixed at a reasonable value.

Here we show results from field application of the cone permeameter. We have modified the method of placement and the test procedure based on previous experience. Before placement of the cone permeameter in the soil, a soil core of smaller diameter was removed with a sampler. This reduced possible disturbances caused by the direct push of the permeameter into the soil. In addition, carefully extracted samples of known volume were used to determine the initial moisture contents of the soil at the tensiometer locations. Initial moisture content values were paired with the corresponding initial tensiometer readings and included in the optimization as points of the soil-moisture characteristic, $\theta(h)$. The cone permeameter infiltration tests were performed immediately after the cone permeameter was placed in the soil and the measured pressure heads reached equilibrium. Tests were always conducted with two sequentially applied pressure heads of different magnitudes for each test. The parameters describing the soil hydraulic properties were estimated from the first part of the experiment alone as a one-step experiment or from both parts as a two-step experiment. Finally, the redistribution, or third part of the experiment, was included in the parameter optimization so that the effects of hysteresis could be studied. The resulting soil hydraulic properties were compared with those determined with standard laboratory and field techniques.

THEORY

Experimental Setup and Problem Definition

A prototype cone permeameter has been discussed in detail by Gribb et al. (1998). A schematic of the device and the experimental setup are shown in Fig. 1. The cone permeameter is placed in the soil, and a known head of water is then supplied to the 5-cm-long screen using a microprocessor-controlled solenoid valve assembly. The cumulative inflow volume infiltrated into the soil through the screen is determined from scale readings of the mass of water removed from the source. Progress of the wetting front is measured with tensiometer rings 5 and 10 cm above the screen. After the water supply valve is closed, the tensiometers monitor the redistribution of water in the soil profile.

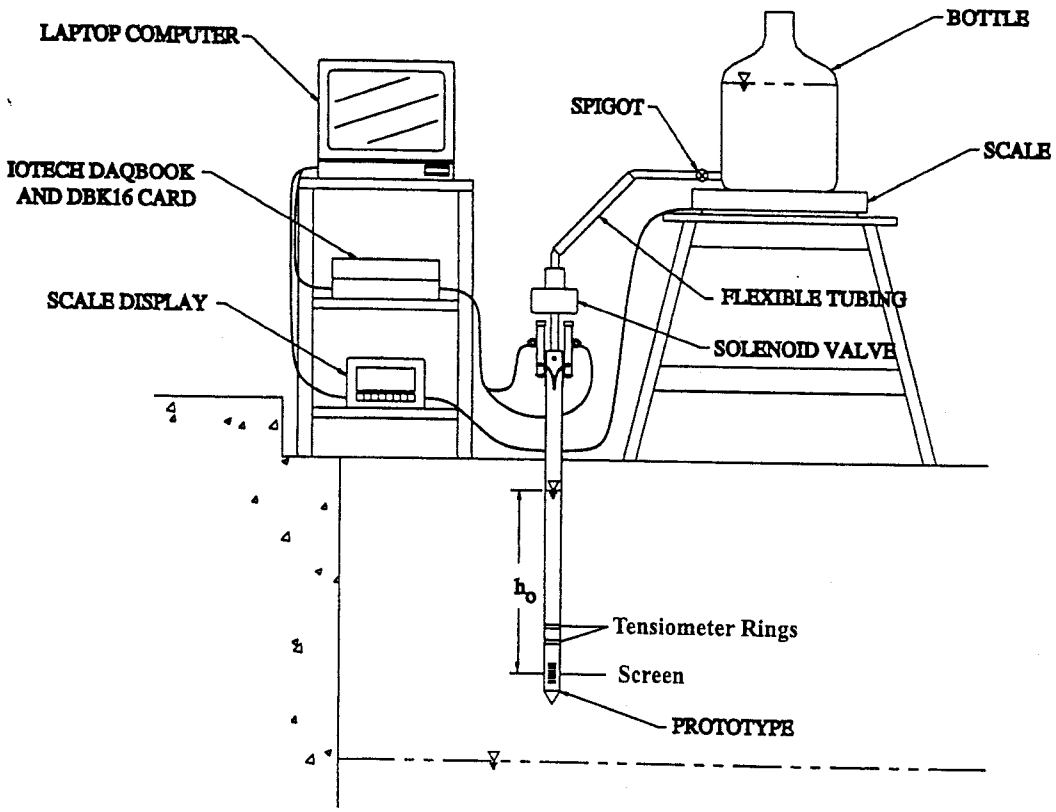

Fig. 1. Cone permeameter test set up.

The cumulative inflow and pressure head data are then analyzed to obtain estimates of $\theta(h)$ and $K(h)$ functions. The flow responses are modeled with an appropriate, variably saturated flow equation, augmented with parameterized hydraulic functions of $K(h)$ and $\theta(h)$, and suitable initial and boundary conditions. The unknown parameters of $K(h)$ and $\theta(h)$ are determined by minimization of an objective function describing the differences between measured flow variables and those simulated with a numerical flow code. During the minimization process the initial parameter estimates are iteratively improved until the desired degree of precision is obtained.

Governing Flow Equation

HYDRUS-2D (Šimůnek et al. 1996) is used to simulate the cone permeameter test in initially unsaturated soil with the finite element discretization of the flow domain shown in Fig. 2. The governing flow equation for radially symmetric, isothermal Darcian flow in an isotropic, rigid porous medium, assuming the air phase plays an insignificant role in the liquid flow process, is (Richards 1931):

$$\frac{\partial \theta}{\partial t} = \frac{1}{r}\frac{\partial}{\partial r}\left[rK\frac{\partial h}{\partial r}\right] + \frac{\partial}{\partial z}\left[K\left(\frac{\partial h}{\partial z} + 1\right)\right] \quad (1)$$

where r is the radial coordinate (L), z is the vertical coordinate positive upward (L), t is time (T), h is the pore water pressure head (L), K is the hydraulic conductivity (LT^{-1}), and θ is the volumetric moisture content (L^3L^{-3}). Eq. (1) is solved numerically for the following boundary and initial conditions:

$$h(r, z, t) = h_i(r, z), t = 0 \quad (2)$$

$$h(r, z, t) = h_0(t) - (z - z_0)$$
$$r = r_0,\ z_0 - \frac{L}{2} < z < z_0 + \frac{L}{2},\ 0 < t < t_w \quad (3)$$

$$v_r(r, z, t) = 0, r = r_0,$$
$$z_0 - \frac{L}{2} < z < z_0 + \frac{L}{2},\ t_w < t < t_r \quad (4)$$

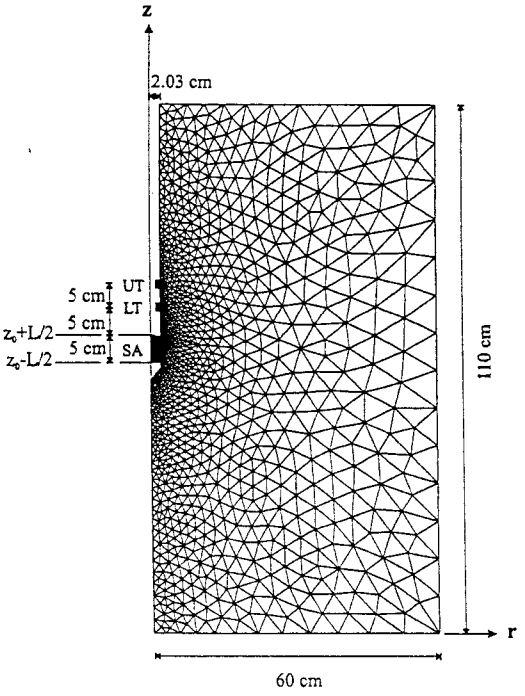

Fig. 2. Finite element discretization of the flow domain used for modeling cone permeameter tests. UT = Upper Tensiometer; LT = Lower Tensiometer; SA = Screened Area.

where h_i is the initial pressure head in the soil (L), h_0 is the supplied pressure head imposed at the center of the screen (L), z_0 is the coordinate of the center of the screen (L), L is the length of the screen, r_0 is the radius of the screen (L), t_w is the time when infiltration is completed (T), t_r is the time when the experiment is terminated (T), and v_r is the flux in the radial direction (LT). Supplied pressure head, h_0, is variable in time and defined as follows:

$$h_0 = h_{0j}, t_{j-1} < t < t_j, j = 1, \ldots, w - 1 \quad (5)$$

$$h_0 = f(V(t)) = f\left(V_{w-1} - \int_{t_{w-1}}^{t} I(t)\,dt\right), t_{w-1} < t < t_w \quad (6)$$

Equation (5) describes a pressure head boundary condition, which can be changed in steps, where h_{0j} (L) is the pressure head applied during the time period $t_{j-1} < t < t_j$, t_j is the time when the applied pressure head h_{0j} is changed, and t_{w-1} is the time when the water supply is shut off and only the water remaining in the cone body infiltrates into the soil. The decreasing actual pressure head during the period $t_{w-1} < t < t_w$, h_0, is calculated with Eq. (6) (based on the geometric characteristics of the interior of the cone body), where V and V_{w-1} (L^3) are the volumes of water at the current time and at the time t_{w-1}, respectively, and I is the actual infiltration rate (L^3T^{-1}) corresponding to the specified boundary conditions. For details, see Šimůnek et al. (1999). The other boundaries are defined as no-flow boundaries.

Unsaturated Soil Hydraulic Properties

The van Genuchten (1980) expressions for moisture content and hydraulic conductivity, $\theta(h)$ and $K(\theta)$, are used in this work:

$$\theta_e = \frac{\theta(h) - \theta_r}{\theta_s - \theta_r} = \frac{1}{(1 + |\alpha h|^n)^m}, h < 0$$
$$\theta_e = 1, h \geq 0 \quad (7)$$

$$K(\theta) = K_s\,\theta_e^l\left[1 - (1 - \theta_e^{1/m})^m\right]^2, h < 0$$
$$K(\theta) = K_s, h \geq 0 \quad (8)$$

where θ_e is the effective moisture content (L^3L^{-3}), K_s is the saturated hydraulic conductivity (LT^{-1}), θ_r and θ_s are the residual and saturated moisture contents (L^3L^{-3}), respectively, l is the pore connectivity parameter (−) ($l = 0.5$), and α (L^{-1}), n and m ($= 1 - 1/n$) are empirical parameters (−).

When the hysteresis of the characteristic curves is taken into account, the drying and wetting curves are described with Eqs. (7) and (8) using the parameter vectors (θ_r^d, θ_s^d, α^d, n^d, K_s^d) and (θ_r^w, θ_s^w, α^w, n^w, K_s^w), respectively, where the superscripts d and w indicate drying and wetting, respectively. Consideration of hysteresis (e.g., description of scanning curves) in the simulation procedure and commonly used restrictions are described in detail by Kool and Parker (1987) and Simùnek et al. (1999). In our study the following simplifications are used:

$$\theta_r^d = \theta_r^w = \theta_r,\ \theta_s^d = \theta_s^w = \theta_s,\ n^d = n^w = n,\ K_s^d = K_s^w = K_s \quad (9)$$

The hydraulic characteristics defined by Eqs. (7) and (8) contain the unknown parameters K_s, θ_r, θ_s, n, α^w, and α^d, which are found by optimization.

Formulation of the Inverse Problem

To derive estimates of the hydraulic parameters using parameter optimization, an objective function, Φ, expressing the differences between flow responses measured with the cone perme-

ameter and those predicted using a numerical model with parameterized soil hydraulic properties, is minimized:

$$\Phi(\boldsymbol{b}, q, p) = \sum_{j=1}^{m_q} v_j \sum_{i=1}^{n_{qi}} w_{i,j} [q^*_j(x, t_i) - q_j(x, t_i, \boldsymbol{b})]^2 + \sum_{j=1}^{m_p} \overline{v}_j \sum_{i=1}^{n_{pj}} \overline{w}_{i,j} [p^*_j(\theta_i) - p_j(\theta_i, \boldsymbol{b})]^2 \quad (10)$$

where the first term on the right side represents deviations between measured and predicted space-time variables (e.g., pressure heads or moisture contents at different locations and/or times, or the cumulative infiltration rate vs. time). In this term, m_q is the number of different sets of measurements, and n_{qj} is the number of measurements in a particular measurement set. Specific measurements at time t_i for the jth measurement set at location $x(r, z)$ are represented by $q_j^*(x, t_i)$; $q_j(x, t_i, \boldsymbol{b})$ are the corresponding model predictions for the vector of optimized parameters $\boldsymbol{b}$ (e.g., θ_r, θ_s, α^w, α^d, n, K_s); and v_j and $w_{i,j}$ are weights associated with a particular measurement set or point, respectively. The weighting factor, v_j, is given by the inverse of the number of measurements multiplied by the variance of those observations, and $w_{i,j}$ is equal to 1 in this work. The second term represents differences between independently measured $p_j^*(\theta_i)$ and predicted $p_j(\theta_i, \boldsymbol{b})$ soil hydraulic properties (e.g., $\theta(h)$, $K(\theta)$ or $K(h)$ data), whereas the terms m_p, n_{pj}, $\overline{v}_j$ and $\overline{w}_{i,j}$ have meanings similar to the first term, but now apply to the soil hydraulic properties.

Minimization of the objective function Φ is accomplished by using the Levenberg-Marquardt nonlinear minimization method (Marquardt 1963), which combines the Newton and steepest descent methods.

MATERIALS AND METHODS

Description of Studied Locations

Tests were carried out at two sites in Poinsett State Park, located southeast of Columbia, South Carolina. This area is composed of interbedded, unconsolidated sands and clays of the Atlantic Coastal Plain (Pitts et al. 1974). Soil profiles in both cases were quite homogeneous and consisted of two layers of sandy soil. Site 1 had a dark grayish-brown surface layer and a pale brown sand subsoil, and Site 2 had a dark reddish-brown surface layer and a darker reddish-brown sand subsoil. The top layers contained organic material and were approximately 10 cm deep. Tests were conducted with the center of the screen at a depth of 50 cm so that the wetting front would not reach the upper organic layer during the experiments. The tested materials had different particle size distributions, as shown in Fig. 3. The soil at Site 2 was more compact and had a higher clay content (5.3% vs. 0.6%), higher silt content (2.3% vs. 1.8%), higher bulk density (1.72 g/cm^3 vs. 1.56 g/cm^3), lower porosity (0.345 vs. 0.4) and, consequently, different hydraulic properties than the soil at Site 1 (See Tables 2 and 3 in Results and Discussion). The hydraulic properties of the soils were determined directly using several standard methods. Capillary rise (Lambe 1951) tests were performed to evaluate the wetting curves of the soil-moisture characteristics. The nonlinear optimization program RETC (van Genuchten et al. 1991) was used to fit $\theta(h)$ data to Eq. (7). Falling head tests (ASTM D-2334) were per-

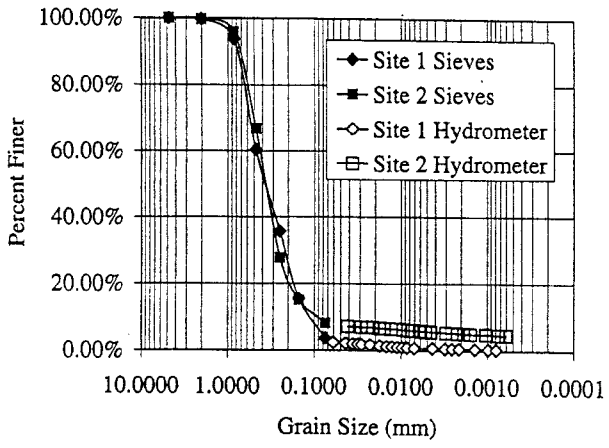

Fig. 3. Grain size distributions for tested materials at Sites 1 and 2 determined via sieve and hydrometer analyses.

formed in the laboratory, and Guelph permeameter tests (Bouwer and Rice 1976) were done *in situ* to obtain the saturated hydraulic conductivity, K_s, of the soil. Multi-step outflow tests (van Dam et al. 1994) on undisturbed soil samples and numerical inversions of observed transient flow data using HYDRUS-1D (Šimůnek et al. 1998c) were carried out to obtain estimates of soil hydraulic parameters describing the drying curves of $\theta(h)$ and $K(h)$. To define soil hydraulic properties accurately in the approximate range of pressure heads measured in the field with the cone permeameter, the multi-step outflow tests were run with the following pressure heads applied at the center of the samples: -10, -25, -55, -100, -170 cm. During each pressure head step, equilibrium was achieved so that the soil moisture contents paired with the applied pressure heads could be included as points of the soil-moisture characteristic in the optimization process. In this case, the pore connectivity parameter, l, was also optimized. Soil samples for laboratory tests were taken close to the screen and tensiometers after the cone permeameter tests were completed. *In situ* Guelph permeameter tests were performed before cone permeameter testing and far enough away so as to not influence the flow region during cone permeameter testing but close enough to obtain properties of approximately the same material.

Cone Permeameter Tests

We performed five tests at different locations at each site. Before the cone permeameter was placed in the soil, a soil core was taken with a sampler of smaller diameter (3.2 cm) than the cone permeameter (4.06 cm). This reduced possible disturbances caused by the direct push of the cone permeameter into the soil. The soil core was divided into sections of known volume, and the initial soil moisture contents were determined. The cone permeameter was then inserted into the sampler hole. Tests were performed immediately after the cone permeameter was placed in the soil, and the measured pressure heads reached equilibrium. Tests were always conducted with two sequentially applied pressure heads. For the first three tests (A, B, and C), pressure heads of 30 and 50 cm were applied to the center of the screen, which corresponded to single-step applied pressure head (30 or 50 cm) experiments performed previously in the laboratory and analyzed by Kodešová et al. (1998, 1999) and Šimůnek et al. (1999). To demonstrate typical flow responses, we show as examples the courses of Tests B at Sites 1 and 2 (Figs. 4a and b). Recorded pressure head changes during the first applied pressure head considerably outweighed changes during the second applied pressure head for both tests (Table 1). To get more significant information about the soil-water regime, it would be more desirable to obtain similar pressure head changes during both steps, with maximum pressure heads close to zero. Therefore, we carried out Tests D with the applied pressure heads of 21 and 108 cm at each site. These pressure heads represent the lowest and highest possible heads that can be supplied with the present prototype. As shown in Figs. 4c and d, the measured pressure change during the first applied pressure step dominated that measured during the second step. In addition, in the case of Test D at Site 2, the overly high applied pressure head and corresponding high flow rate probably disturbed the soil structure, which resulted in a decrease in the initially high infiltration rate, as well as the pressure heads during the second applied pressure head step. Finally we conducted Tests E with applied pressure heads of 21 and 80 cm. The effects of structural changes resulting from the higher applied pressure head is again evident, but appear to be less significant than for Test D (Figs. 4e and f).

Tests were run for different lengths of time according to the measured responses, as shown in Table 1. The total time necessary to perform a prototype test is increased by the time required for test preparation, which depends on the technique used. We are currently using a rack jack assembly (Geonor Inc.). This involves placement of soil anchors, after which the insertion frame must be secured, and, finally, the soil sampler and the cone permeameter can be pushed into the soil. This takes approximately 40 min. It takes another 10 min. to assemble the cone permeameter set up as shown in Fig. 1.

Inverse Solutions

Cone permeameter experiments with only one applied pressure head were analyzed in previous studies (Gribb et al. 1998; Kodešová et al. 1998, 1999; Šimůnek et al. 1999). Therefore, we performed numerical inversions for data (cumulative inflow, upper and lower tensiometer pressure heads) collected during the first infiltration part of the experiments, e.g., for applied pressure heads of 30 (Tests A, B, and C) or 21 cm (Tests D and E). To study the effect of the second applied pressure head on estimates of the soil hydraulic properties, we then carried out numerical inver-

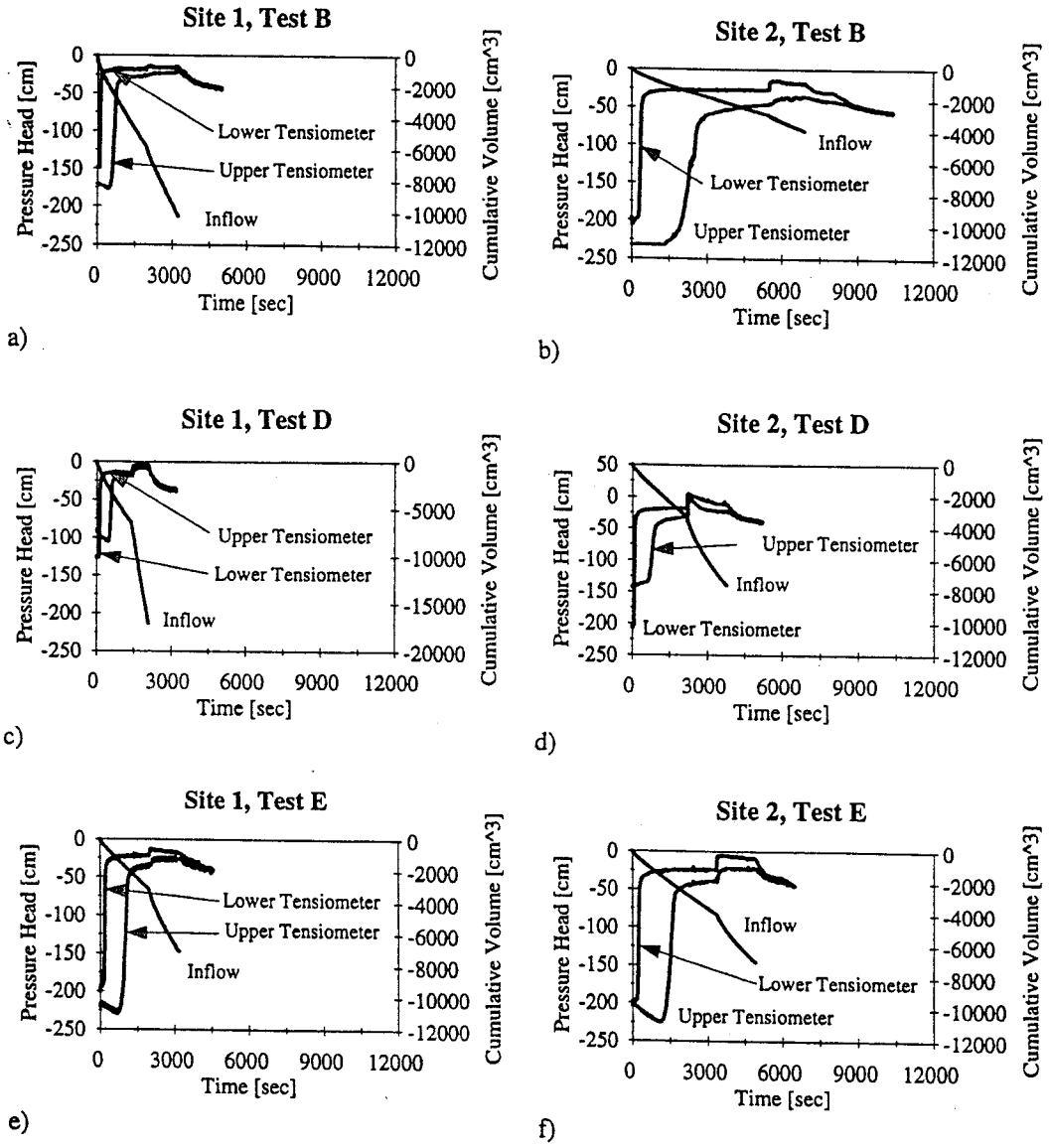

Fig. 4. Observed cumulative inflow volumes and pressure heads for Tests B, D and E at Sites 1 and 2.

sions for data collected during both the first and second parts of the experiments with applied pressure heads of 30 and 50 cm (Tests A, B, and C), or 21 and 108 cm (Test D at Site 1 only), or 21 and 80 cm (Test E). Test D at Site 2 was not analyzed because of soil structural changes that occurred during the second pressure head step. Finally, for selected tests we analyzed data from the entire experiment (e.g., the wetting and redistribution parts) to study hysteresis of the soil hydraulic properties. In all cases, the initial soil moisture content determined at the position of the upper tensiometer was paired with the initial pressure head reading and included in the optimization using the second term of Eq. (10).

Initial pressure heads in the domain were set equal to the initial upper tensiometer reading for elevations at or above that of the upper tensiometer. Similarly, the pressure heads at the elevation of the lower tensiometer or below were set equal to the lower tensiometer initial reading. The pressure heads between the two tensiometers were linearly distributed. The external boundaries were set as no-flow boundaries. The

TABLE 1

Observed pressure heads at the lower tensiometer (LT), upper tensiometer (UT), and the cumulative inflow volume (CI) at the beginning and end of each step

Tests	Initial measurements			Measurements at end of 1st step (1st Applied Pressure Head)				Measurements at end of 2nd step (2nd Applied Pressure Head)				Measurements at end of the 3rd step (Redistribution)		
	Time (s)	LT (cm)	UT (cm)	Time (s)	LT (cm)	UT (cm)	CI (cm^3)	Time (s)	LT (cm)	UT (cm)	CI (cm^3)	Time (s)	LT (cm)	UT (cm)
A, Site 1	0	−150	−174	1210	−19	−24	4598	1860	−19 (−16)*	−21	7272	4010	−45	−43
B, Site 1	0	−148	−170	1970	−18	−26	5746	3260	−14	−21	10236	5020	−42	−44
C, Site 1	0	−192	−231	2530	−21	−26	5324	3890	−22 (−19)*	−25 (−24)*	8850	6390	−50	−46
D, Site 1	0	−126	−93	1400	−15	−19	6678	2100	−3	−7	17044	3200	−38	−36
E, Site 1	0	−200	−216	1980	−22	−34	3164	3180	−18 (−12)*	−25	7050	4560	−39	−40
A, Site 2	0	−173	−200	1960	−17	−36	2238	3080	−8 (−5)*	−26 (−25)*	3804	4940	−56	−57
B, Site 2	0	−202	−232	5500	−26	−45	2836	6900	−17 (−14)*	−35	3846	10400	−55	−56
C, Site 2	0	−213	−232	5120	−29	−48	3200	6800	−22	−39	4540	9040	−53	−56
D, Site 2	0	−202	−141	2180	−19	−32	3270	3780	−12 (+4)*	−23 (−4)*	7582	5200	−38	−40
E, Site 2	0	−200	−201	3360	−24	−38	3958	4920	−10 (−5)*	−22	6990	6500	−44	−44

*The maximum pressure head observed immediately after the application of the second, higher pressure head.

screen was modeled as a constant head boundary, with water pressure head ranging from 27.5 to 32.5 cm (or 18.5 to 23.5 cm) from bottom to top for the first step and from 47.5 to 52.5 cm (or 105.5 to 110.5 cm or 77.5 to 82.5 cm) for the second step. For the third (redistribution) part of the experiment, the screen was defined as a known head boundary, described by Eq. (3) for the initial infiltration of water remaining in the cone body after the water supply was shut off and then as a no-flow boundary after the cone was empty.

All inverse solutions were obtained with the same sets of optimized parameters, θ_r, θ_s, α^w, n and K_s. When we considered hysteresis, the parameter α^d was also estimated. It must be mentioned that it is only possible to estimate both parameters, θ_r and θ_s, when the initial soil moisture content is included in the optimization process. Without this information, one of these parameters must be set at a reasonable value, and only one can be optimized from analysis of our test data. Initial estimates for results shown here were always set as follows: $\theta_r = 0.09$; $\theta_s = 0.38$; $\alpha^w = 0.035\ cm^{-1}$; $n = 4.0$; $K_s = 0.002$ cm/sec; and $\alpha^d = 0.035\ cm^{-1}$. We restricted parameter n to the range of 2.01 to 7 (or 2.01 to 5 for Tests A and D at Site 2) and parameter θ_s to the range of 0.2 to 0.6. To investigate the uniqueness of the optimized parameters, we also carried out inversions for some tests with different initial estimates of the hydraulic parameters. We obtained almost the same results, without significant deviations. On the other hand, we had to restrict parameter n to < 5 due to nonconvergence of solution in the two cases noted above.

The computational time required for inverse solution depended on the length of the test, the initial parameter estimates, and the efficiency of the computer. In our case, it took from 1 to 5 hours to analyze the two-step tests and from 2 to 10 hours for the entire experiment on a Pentium II Pro 200 MHz.

RESULTS AND DISCUSSIONS

The soil hydraulic parameters obtained from all numerical inversions of cone permeameter data and those obtained using standard techniques are presented in Tables 2 and 3 and in Fig. 8. Measured and simulated cumulative flow and pressure head data are shown for Tests B and E from both sites in Figs. 5, 6, and 7.

One-step Pressure Head Experiments

Figures 5a–5d show the results of analysis for the one-step pressure head experiments: Test

TABLE 2

Hydraulic parameters α^w, α^d, n, θ_r, θ_s and K_s obtained from different tests at Site 1, where the measured bulk densities and porosities ranged between 1.45 and 1.70 g/cm³, and 0.350 and 0.458, respectively

Test method	Hydraulic parameters				
	α^w (α^w/α^d (cm^{-1}))	n (−)	θ_r (−)	θ_s (−)	K_s (cm/sec)
Capillary Rise (1 of 2 Columns)	0.067	2.10	0.000	0.380	—
Multi-Step Outflow (1 of 2 Samples)*	0.028	3.86	0.140	0.400	0.0014
Guelph Permeameter (4 Test Holes)					0.0025–0.0038
Laboratory Falling Head (9 Samples)					0.0013–0.0044
Cone Permeameter A, h_0 = 30 cm	0.037	3.97	0.088	0.379	0.0022
Cone Permeameter A, h_0 = 30, 50 cm	0.035	4.81	0.089	0.377	0.0020
Cone Permeameter B, h_0 = 30 cm	0.037	3.95	0.088	0.400	0.0018
Cone Permeameter B, h_0 = 30, 50 cm	0.035	4.79	0.089	0.393	0.0016
Cone Permeameter B, h_0 = 30, 50 cm, & redistribution	0.035/0.026	4.46	0.088	0.390	0.0016
Cone Permeameter C, h_0 = 30 cm	0.034	3.65	0.082	0.433	0.0011
Cone Permeameter C, h_0 = 30, 50 cm	0.033	4.04	0.083	0.449	0.0011
Cone Permeameter D, h_0 = 21 cm	0.047	2.53	0.055	0.443	0.0040
Cone Permeameter D, h_0 = 21, 108 cm	0.044	3.11	0.069	0.447	0.0036
Cone Permeameter E, h_0 = 21 cm	0.035	3.19	0.087	0.333	0.0011
Cone Permeameter E, h_0 = 21, 80 cm	0.031	4.09	0.089	0.350	0.0010
Cone Permeameter E, h_0 = 21, 80 cm, & redistribution	0.031/0.026	4.02	0.089	0.349	0.0010

*Pore connectivity parameter, l, in Eq. (8) was also optimized (l = − 1.57).

B—Site 1 (Fig. 5a), Test B—Site 2 (Fig. 5b), Test E—Site 1 (Fig. 5c), and Test E—Site 2 (Fig. 5d). In all cases, the cumulative inflows were well simulated. Optimized pressure heads corresponded closely with observed values, except for the part when pressure heads measured with the upper tensiometer approached their final values (Figs. 5a, c, and d) for the initial increase of pressure head at the upper tensiometer (Fig. 5b). The simulations did not match the initial decreases of pressure heads measured with the upper tensiometer (c and d). These measured pressure head declines were probably caused by air that was forced ahead of the wetting front and, as such,

TABLE 3

Hydraulic parameters α^w, α^d, n, θ_r, θ_s and K_s obtained from different tests at Site 2, where the measured bulk densities and porosities ranged between 1.61 and 1.85 g/cm³, and 0.304 and 0.391, respectively

Test method	Hydraulic parameters				
	α^w (α^w/α^d) (cm^{-1})	n (−)	θ_r (−)	θ_s (−)	K_s (cm/sec)
Capillary Rise (1 of 2 Columns)	0.052	2.20	0.055	0.380	
Multi-Step Outflow (1 of 2 Samples)*	0.018	3.46	0.134	0.350	0.00013
Guelph Permeameter (4 Test Holes)					0.00044–0.00075
Laboratory Falling Head (6 Samples)					0.00011–0.00064
Cone Permeameter A, h_0 = 30 cm	0.030	5.00	0.176	0.309	0.00061
Cone Permeameter A, h_0 = 30, 50 cm	0.031	4.98	0.176	0.303	0.00061
Cone Permeameter B, h_0 = 30 cm	0.026	5.29	0.124	0.331	0.00025
Cone Permeameter B, h_0 = 30, 50 cm	0.026	5.07	0.124	0.328	0.00025
Cone Permeameter B, h_0 = 30, 50 cm, & redistribution	0.025/0.018	4.05	0.120	0.321	0.00026
Cone Permeameter C, h_0 = 30 cm	0.022	3.18	0.142	0.385	0.00030
Cone Permeameter C, h_0 = 30, 50 cm	0.022	3.24	0.143	0.386	0.00029
Cone Permeameter D, h_0 = 21 cm	0.036	5.00	0.120	0.303	0.00096
Cone Permeameter D, h_0 = 21, 108 cm					
Cone Permeameter E, h_0 = 21 cm	0.032	4.07	0.099	0.385	0.00074
Cone Permeameter E, h_0 = 21, 80 cm	0.031	4.96	0.099	0.381	0.00067
Cone Permeameter E, h_0 = 21, 80 cm, & redistribution	0.031/0.024	4.89	0.099	0.381	0.00066

*Pore connectivity parameter, l, in Eq. (8) was also optimized (l = − 2.38).

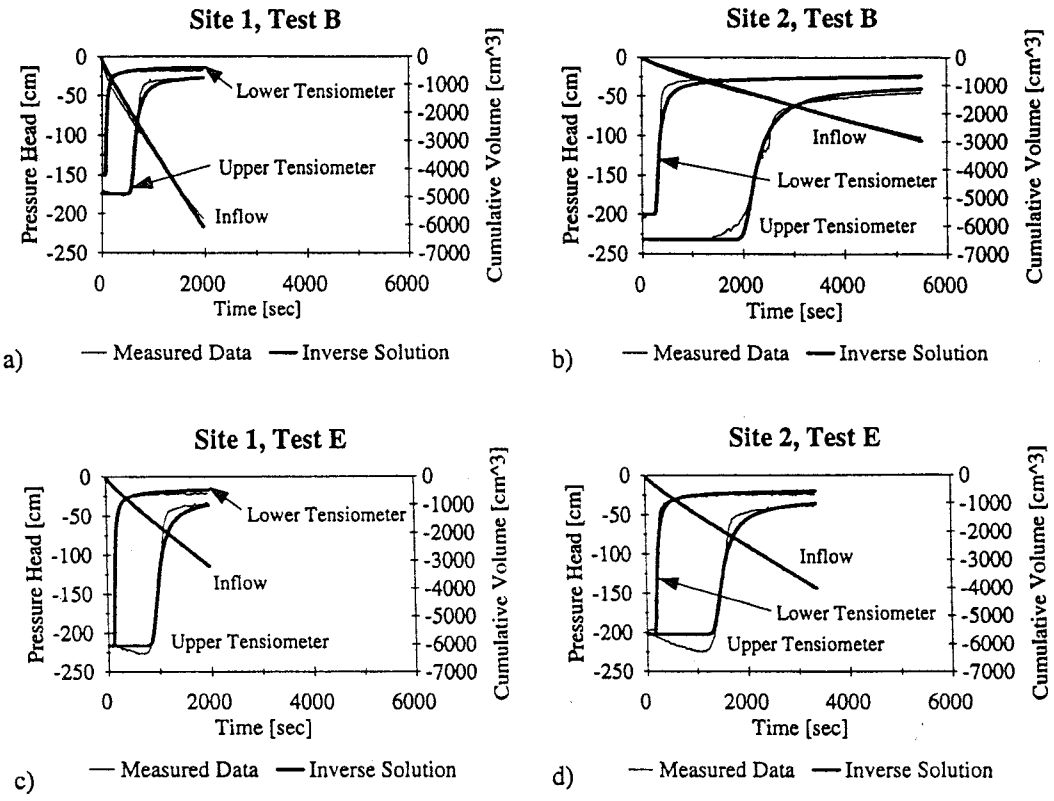

Fig. 5. Observed data and simulated cumulative inflow volumes and pressure heads resulting from analysis of first infiltration part of experiments with one applied pressure head; h_0 = 30 cm for Tests B at Sites 1 and 2, and h_0 = 21 cm for Tests E at Sites 1 and 2.

cannot be described with the numerical model. The pressure changes at these low pressure heads correspond to a very small change in moisture content for these soils. Therefore, we assumed that the air phase had little influence on the water flow regime.

The soil hydraulic properties estimated from all cone permeameter experiments at Site 1 were very similar (Table 2). At Site 2, the estimated properties varied to some degree, but such variability was also observed using the other experimental techniques (Table 3). This suggests that the proposed cone permeameter method provided consistent results. Inclusion of the initial moisture content in the objective function yielded realistic estimates of θ_s values that corresponded well to measured porosities.

Two-Step Pressure Head Experiments

Fig. 6a–6d shows the results of analysis for the two-step pressure head experiments: Test B—Site 1 (Fig. 6a), Test B—Site 2 (Fig. 6b), Test E—Site 1 (Fig. 6c), and Test E—Site 2 (Fig. 6d). Cumulative inflows were again well simulated. Modeled pressure heads during the first step responded in the same way as for the one-step experiments. Simulated pressure heads during the second step followed measured data from the upper tensiometer better than those from the lower one. Logically, the simulations did not reproduce the initial increase and subsequent decline in the pressure heads observed after application of the second pressure head. The pressure decrease was more obvious for the lower tensiometer. As discussed previously, this was likely caused by soil structural changes.

In previous studies, higher values of θ_s and K_s were obtained for one-step experiments with higher applied pressure heads (50 cm) than for experiments with lower applied pressure heads (30 cm) (Kodešová et al. 1998, 1999; Šimůnek et al. 1999). A similar effect was not found in this work. The application of higher pressure heads in the two-step experiments did not influence the resulting soil hydraulic properties greatly when compared with those obtained from the one-step

experiments (Tables 2 and 3). Of course, the results from the two-step experiments were still controlled mainly by the first steps. However the measured data during the second step were tracked well, especially the cumulative inflows, which primarily influenced values of K_s. The benefit of performing and analyzing two-step experiments (even with such small impacts on observed pressure heads during the second part) was that the inverse problem was better defined, thus preventing the inverse algorithm from wandering into areas of parameter space that could cause numerical instabilities. When analyzing the one-step experiments, the inverse algorithm attempted several times to make a step in the direction of the n parameter (if unconstrained) that resulted in numerical instabilities (Site 2, Tests A and D). Better definition of the inverse problem also improved the stability of the inverse solution. Since the higher supply pressure heads during the second step extended the ranges of measured pressure heads at both tensiometer rings (Table 1), the optimized parameters are expected to be representative for wider ranges of pressure heads. In addition, the optimized hydraulic properties better define behavior near saturation. The accurate description of the soil hydraulic properties close to saturation has recently received much attention (van Genuchten and Leij 1999).

Three-Step Experiment (Two Applied Pressure Heads and Redistribution)

Figures 7a through 7d show the results of analysis for the three-step pressure head experiments: Test B—Site 1 (Fig. 7a), Test B—Site 2 (Fig. 7b), Test E—Site 1 (Fig. 7c), and Test E—Site 2 (Fig. 7d). The simulated flow responses during the first and second parts of the experiment were similar to those obtained for the two-step experiment. The pressure heads during the redistribution part were modeled satisfactorily, except for the pressure heads measured with the lower tensiometer for Test B at Site 2. In this case, the measured pressure heads decreased in two steps. The numerical model with the prescribed boundary conditions could not simulate such behavior.

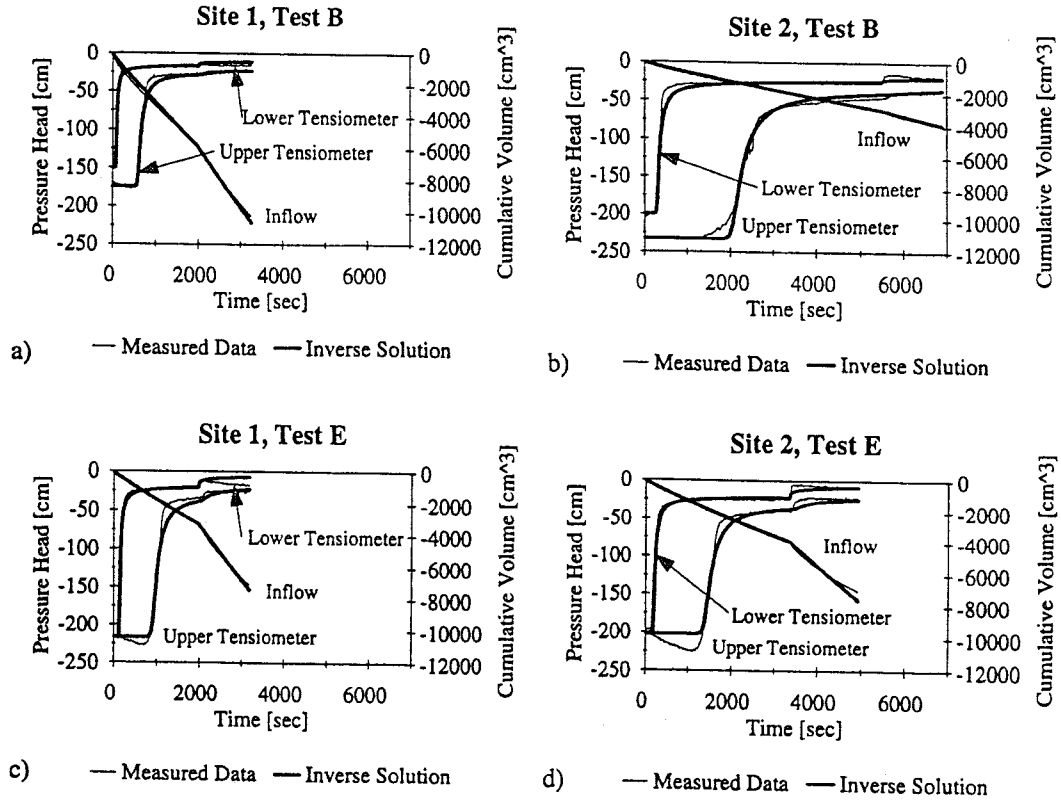

Fig. 6. Observed data and simulated cumulative flow volumes and pressure heads resulted from analysis of first and second infiltration parts of experiments with two applied pressure heads; h_0 = 30 and 50 cm for Tests B at Site 1 and 2, and h_0 = 21 and 80 cm for Tests E at Site 1 and 2.

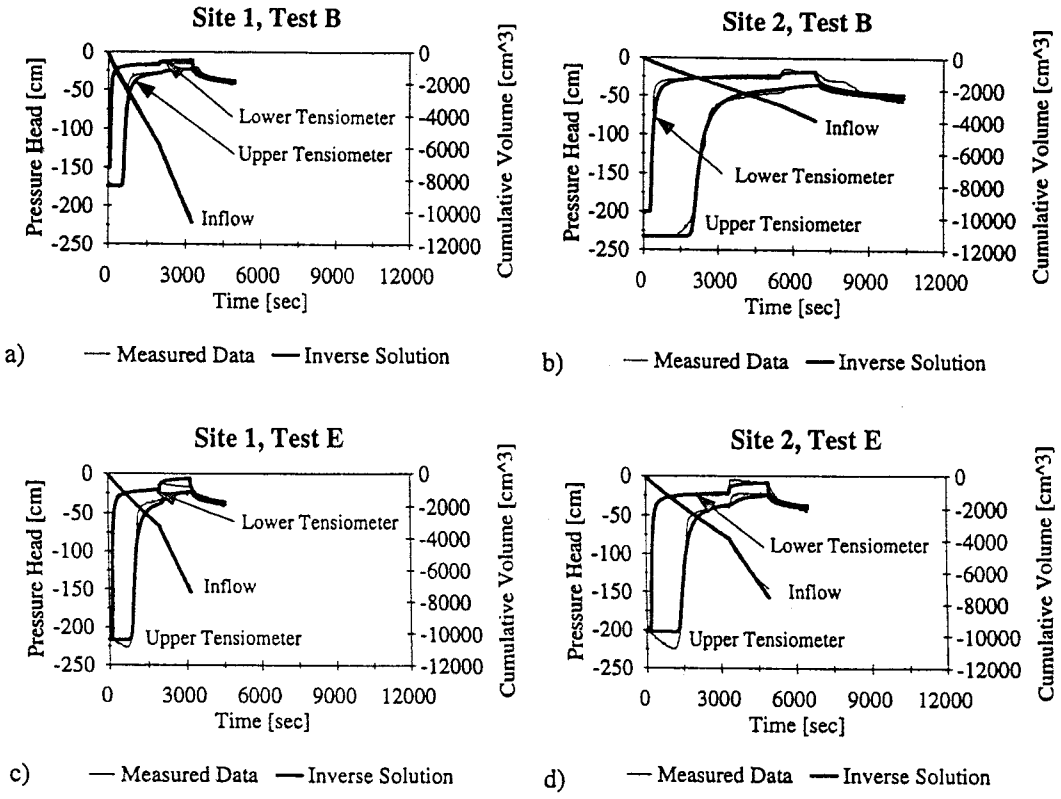

Fig. 7. Observed data and simulated cumulative inflow volumes and pressure heads resulting from analysis of the first and second infiltration parts of experiments with two applied pressure heads, h_0 = 30 and 50 for Tests B at Sites 1 and 2, and h_0 = 21 and 80 cm for Tests E at Sites 1 and 2, and the third redistribution part with no infiltration through the screen.

The pressure head decreases for all cases during the water redistribution process were small compared with the total pressure head increases during the infiltration parts of the experiments. Thus, it would seem that the information obtained would be less significant. However, the inverse solutions did yield reasonable estimates of parameter α^d defining the drying process, and the resulting soil hydraulic properties characterizing the wetting curves were almost the same as for the two-step experiment (Tables 2 and 3). The different α parameters for the wetting and drying curves illustrated hysteresis (Fig. 8).

Comparison of Soil Hydraulic Properties Obtained via Inverse Solutions and Other Techniques

Soil-moisture characteristics obtained with numerical inversions correspond well with those measured with the multi-step outflow technique describing drying curves and satisfactorily with the curves from the capillary rise tests characterizing the wetting curves (Fig. 8). It must be noted that the capillary rise tests were performed on repacked soil columns. To measure properties similar to those determined on undisturbed samples, it is necessary to ensure the same density of material. This was difficult to achieve (especially in the case of the soil from Site 2), and, as a result, higher saturated soil moisture contents were obtained. In addition, the soils were initially very dry, and, therefore, the data obtained described the limiting wetting curves, and the optimized residual soil-moisture contents were lower than those determined by the other methods. On the other hand, the residual soil moisture contents from the multi-step outflow tests were higher than those obtained from the other tests. Multi-step outflow tests were performed with pressure heads ranging between 0 and −170 cm, and the determined parameters are characteristic for that range. It is probable that the value of θ_r would be lower if tests were run for lower pressure heads. Nonetheless, the curves predicted by inversion of cone permeameter data lie predominantly be-

tween multi-step outflow and capillary rise curves.

The estimated saturated hydraulic conductivities were in the range of measured data obtained with the laboratory falling head test and near the lower limit of values obtained with the Guelph permeameter in the field. We consider such correspondence to be excellent.

CONCLUSION

In this article we document the applicability of a prototype cone permeameter for determining hydraulic properties of sandy soil in the field. The tested materials (the second layers of the soil profiles) were very homogeneous, without obvious layering or anisotropy, and, as a result, optimization of parameters θ_r, θ_s, α^w, α^d, n, and K_s was sufficient for describing the observed flow responses. The solution, including anisotropy, was previously discussed by Šimůnek et al. (1999) and Kodešová et al., (1999). Analysis of cone permeameter tests in an anisotropic laboratory aquifer soil returned unreasonably high estimates of θ_s. They found that an anisotropy factor expressing the relationship between horizontal and vertical hydraulic conductivities could be optimized to obtain good agreement between observed and simulated flow responses if θ_s was fixed at a reasonable value.

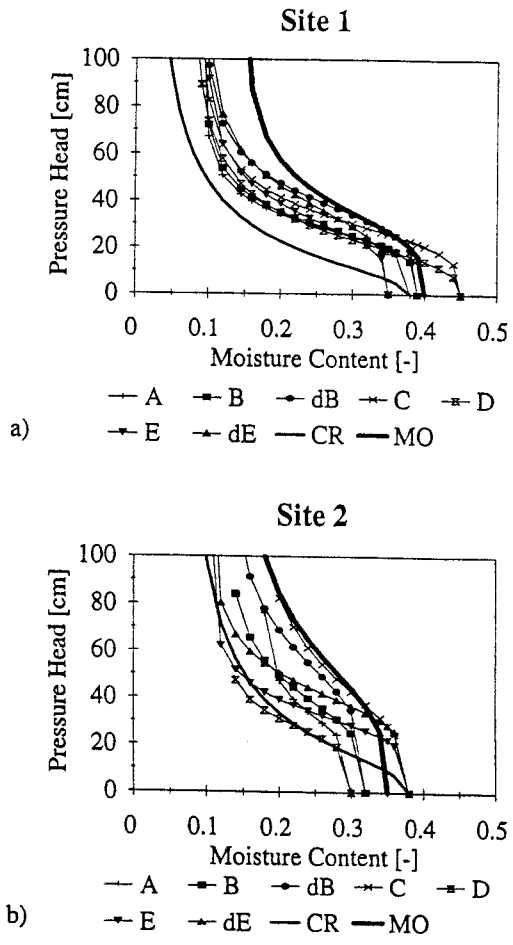

Fig. 8. Soil-moisture characteristic curves obtained with standard methods and those obtained from inverse solutions for all tests. Only the curves resulting from analysis of the following data are presented: Test D at Site 2 (one-step); Tests A, C, and D at Site 1, and Tests A and C at Site 2 (two-step); and Tests B and E at Sites 1 and 2 (three-step), where dB and dE refer to the drying curves. CR and MO refer to the curves obtained from the capillary rise and multi-step outflow experiments, respectively.

The technique for obtaining the initial moisture content of the soil and use of this information in the optimization process proved to be very useful. Inclusion of the initial moisture content, paired with the initial tensiometer reading, allowed for realistic estimation of θ_r and θ_s values. Without this information, only one of these parameters can be optimized, and the other one must be set at a reasonable value for our experimental data sets. Analysis of one- and two-step tests yielded similar parameters, presumably because of the dominant influence of the first step on the inverse solutions. However, addition of the second step better defined the inverse problem, stabilized the numerical and inverse solutions, and resulted in parameters representative of a wider range of pressure heads. Application of higher applied pressure heads to force pressure head readings closer to saturation was problematic. The higher flow likely caused destruction of the existing soil structure and, consequently, changed the soil properties. Thus, we do not recommend use of applied pressure heads higher than 80 cm with this device. The wetting hydraulic parameters obtained from analysis of the entire experiments were consistent with those obtained from analysis of only the wetting parts of the two-step experiments. The drying α (α^d) was lower, as expected. The different α values described the effect of hysteresis. The estimated hydraulic properties corresponded well with those obtained with standard techniques.

We have studied application of parameter estimation to cone permeameter data in different sandy soils, and for this type of soil, this experimental technique seems to be fully applicable. Future work will include field studies in other soil types.

ACKNOWLEDGMENTS

The authors thank S. Anderson and M. Mwamba for performing some of the laboratory tests, and the National Science Foundation CAREER Grant CMS-9501772 and U.S. Army Research Office Grant DAAH04-95-1-0228 for support of this project. The authors also acknowledge the anonymous reviewers.

REFERENCES

Bohne, K., C. Roth, F. J. Leij, and M. Th. van Genuchten. 1993. Rapid method for estimating the unsaturated hydraulic conductivity from infiltration measurement. Soil Sci. 155:237–244.

Bouwer, H., and R. C. Rice. 1976. A slug test for determining hydraulic conductivity of unconfined aquifers with completely or partially penetrating wells. Water Resour. Res. 12:423–428.

Ciollaro, G., and N. Romano. 1995. Spatial variability of the soil hydraulic properties of a volcanic soil. Geoderma 65:263–282.

Eching, S. O., and J. W. Hopmans. 1993. Optimization of hydraulic functions from transient outflow and soil water pressure data. Soil Sci. Soc. Am. J. 57:1167–1175.

Eching, S. O., J. W. Hopmans, and O. Wendroth. 1994. Unsaturated hydraulic conductivity from transient multi-step outflow and soil water pressure data. Soil. Sci. Soc. Am. J. 58:687–695.

Gribb, M. M. 1996. Parameter estimation for determining hydraulic properties of a fine sand from transient flow measurements. Water Resour. Res. 32:1965–1974.

Gribb, M. M., J. Šimůnek, and M. F. Leonard. 1998. Use of a cone penetrometer method to determine soil hydraulic properties. J Geotech. Geoenviron. Eng. 124:820–829.

Inoue, M., J. Šimůnek, J. W. Hopmans, and V. Clausnitzer. 1998. In-situ estimation of soil hydraulic functions using a multi-step soil-water extraction technique. Water Resour. Res. 34:1035–1050.

Kodešová, R., M. M. Gribb, and J. Šimůnek. 1998. Estimating soil hydraulic properties from transient cone permeameter data. Soil Sci. 163:436–453.

Kodešová, R., M. M. Gribb, and J. Šimůnek. 1999. Use of the cone permeameter method to determine soil hydraulic properties. *In* Characterization and Measurement of the Hydraulic Properties of Unsaturated Porous Media. M. Th. van Genuchten and F. J. Leij (eds.). University of California, Riverside.

Kool, J. B., and J. C. Parker. 1987. Development and evaluation of closed-form expressions for hysteretic soil hydraulic properties. Water Resour. Res. 23:105–114.

Kool, J. B., J. C. Parker, and M. Th. Van Genuchten. 1987. Parameter estimation for unsaturated flow and transport models—A review. J. Hydrol. 91:255–293.

Kool, J. B., J. C. Parker, and M. Th. van Genuchten. 1985. Determining soil hydraulic properties from one step outflow experiments by parameter estimation: I. Theory and numerical studies. Soils Sci. Soc. Am. J. 49:1348–1354.

Lambe, W. T. 1951. Capillary phenomena in cohesionless soils. Trans. ASCE 116:401–423.

Leonard, M. F. 1997. Design and laboratory evaluation of a cone permeameter for unsaturated soil hydraulic parameter determination. MS thesis, Univ. of South Carolina, Columbia, SC.

Marquardt, D. W. 1963. An algorithm for least-squares estimation of non-linear parameters. SIAM J. Appl. Math. 11:431–441.

Parker, J. C., J. B. Kool, and M. Th. van Genuchten. 1985. Determining soil properties from one-step outflow experiments by parameter estimation, II. Experimental studies. Soil Sci. Soc. Am. J. 49: 1354–1359.

Pitts, J. J., F. L. Green, and T. R. Gerald. 1974. Soil Survey of Florence and Sumter Counties, South Carolina. United States Dept. of Agriculture, Soil Conservation Service, in cooperation with South Carolina Agricultural Experimental Station, Washington DC.

Richards, L. A. 1931. Capillary conduction of liquids through porous mediums. Physics 1:318–333.

Russo, D., E. Bresler, U. Shani, and J. C. Parker. 1991. Analyses of infiltration events in relation to determining soil hydraulic properties by inverse-problems methodology. Water Resour. Res. 27:1361–1373.

Santini, A., N. Romano, G. Ciollaro, and V. Comegna. 1995. Evaluation of a laboratory inverse method for determining unsaturated hydraulic properties of a soil under different tillage practices. Soil Sci. 160:340–351.

Šimůnek, J., M. Šejna, and M. Th. van Genuchten. 1996. HYDRUS-2D, Simulation Water Flow and Solute Transport in Two-Dimensional Variably Saturated Media. Version 1.0, IGWMC-TPS-53. International Groundwater Modeling Center, Colorado School of Mines, Golden, CO.

Šimůnek J., and M. Th. van Genuchten. 1996. Estimating unsaturated soil hydraulic properties from tension disk infiltrometer data by numerical inversion. Water Resour. Res. 32:2683–2696.

Šimůnek, J., and M. Th. van Genuchten. 1997. Estimating unsaturated soil parameters from multiple tension disc infiltrometer data. Soil Sci. 162: 383–398.

Šimůnek, J., D. Wang, P. J. Shouse, and M. Th. van Genuchten. 1998a. Analysis of a field tension disc infiltrometer experiment by parameter estimation. Int. Agrophys. 12:167–180.

Šimůnek, J., O. Wendroth, and M. Th. van Genuchten. 1998b. A parameter estimation analysis of the evaporation method for determining soil hydraulic properties. Soil Sci. Soc. Am. J. 62:894–905.

Šimůnek, J., M. Šejna, K. Huang, and M. Th. van Genuchten. 1998c. HYDRUS-1D for Windows. Simulating the one-dimensional movement of water, heat and solute movement in variably saturated media. Version 1.0, IGWMC-TPS-70. Interna-

tional Ground Water Modeling Center, Colorado School of Mines, Golden, CO.

Šimůnek, J., R. Kodešová, M. M. Gribb, and M. Th. van Genuchten. 1999. Estimating hysteresis in the soil water retention function from cone permeameter test data. Water Resour. Res. 35:1329–1345.

van Dam, J. C., N. M. Stricker, and P. Droogers. 1992. Inverse method for determining soil hydraulic functions from one-step outflow experiments. Soil Sci. Soc. Am. J. 56:1042–1050.

van Dam, J. C., N. M. Stricker, and P. Droogers. 1994. Inverse method to determine soil hydraulic functions from multi-step outflow experiments. Soil Sci. Soc. Am. J. 58:647–652.

van Genuchten, M. Th. 1980. A closed-form equation for predicting the hydraulic conductivity of unsaturated soils. Soil Sci. Soc. Am. J. 44:892–898.

van Genuchten, M. Th., and F. J. Leij (eds.). 1999. Characterization and Measurement of the Hydraulic Properties of Unsaturated Porous Media. University of California, Riverside, CA.

Wildenschild, D., K. Hìgh Jensen, K. J. Hollenbeck, T. H. Illangasekare, D. Znidarcic, T. Sonnenborg, and M. B. Butts. 1997. A two-stage procedure for determining unsaturated hydraulic characteristics using a syringe pump and outflow observation. Soil Sci. Soc. Am. J. 61:347–359.

Zurmühl, T., and W. Durner. 1998. Determination of parameters for bimodal hydraulic function by inverse modeling. Soil Sci. Soc. Am. J. 62:874–880.